Heteropolyacid and Lithium Infused Calcium Oxide Catalyst for Biodiesel Production from Food Waste

Alisha Kakkar[*,iD] and Sudesh Kumar[iD]

Department of Chemistry, Banasthali Vidyapith, Banasthali-304022, India

*Corresponding author: E-mail: alisha.mcmdav@gmail.com

The advancement of mixed metal oxide catalysts has attracted considerable attention among various workers. Supported MoOx catalyst materials possess more Lewis and Brønsted acid functionalities which assist in the efficient biodiesel production. In this study, ammonium molybdate and Li$^+$ were loaded over eggshells-derived calcium oxide to transesterify the frying oil/waste cooking oil (WCO) to produce biodiesel/fatty acid methyl ester (FAME). Characterization techniques *i.e.*, X-ray diffraction (XRD), scanning electron microscopy (SEM) and Fourier transform infrared spectroscopy (FTIR) analysis were employed to confirm the material. The surface modelling predicted the transesterification reaction parameters. The optimal condition to transesterify WCO with synthesized Mo/Li/CaO catalyst was 6 wt.% catalyst dose, 13.70:1 ratio of methanol:oil (m/o), time of 1 h and 60 ºC temperature. The optimum FAME yield of 97% was observed. The gas chromatography-mass spectroscopy (GC-MS) and other spectroscopic techniques were used to analyze produced FAME. The reusability of catalyst was good and the catalyst can be reutilized effectively up to a limit of 5 runs. By leveraging this innovative catalyst derived from eggshells, this study contribute to a more sustainable and cost-effective biodiesel production process.

Keywords: Ammonium molybdate, Biodiesel, Calcium oxide, Catalysis, Eggshells, Fatty acids, Heterogeneous catalysis.

INTRODUCTION

Hydrocarbon fuels are vital energy providers in contemporary living [1]. However, the demand for fuel is increasing rapidly worldwide. Economical and sustainable energy sources are regarded as crucial features of modern society. Non-renewable energy sources, like petroleum and coal, are being depleted at an alarming rate due to their widespread use. Also, the surge in vehicles has led to environmental degradation and health problems due to greenhouse gas and other pollutant emissions. Biodiesel has been considered a viable energy reservoir over the last decade. The diesel engine generates black carbon soot, which is toxic to the environment, but biodiesel is a clean fuel. Biodiesel can be employed in its unadulterated state or combined with conventional petroleum fuel, from additive levels to 100%, to improve the engine's efficiency and minimize gaseous emissions. The harmful emissions get reduced when blended with biodiesel and are related to the amount of biodiesel in blend.

Fatty acid methyl esters are the best substitutes for traditional fossils, which are cost-effective as well as a potential energy source for the future due to their ecological advantages like renewability, sustainability, low inflammability, decomposability, high flash point, high combustion efficiency and non-toxicity [2]. Various edible oils like soybean, rapeseed, palm, coconut and olive oil and so on and inedible oils like rubber seed oil, jatropha, Karanja, castor oil, *etc.*, have been utilized to generate FAME. Others, like used vegetable oil and oil derived from microalgae, *etc.* have also been utilized for biodiesel generation [3,4]. Vegetable oil is mainly utilized in methyl ester production because it is easily accessible but increases the price and demand for edible oils. Waste cooking oil (WCO) can be sourced from various origins like residential households, restaurants and industries. The disposal of WCO raises specific problems, *e.g.* blockage of pipes when the oil solidifies [5]. Using WCO in biodiesel production reduces the government's work in waste management and protects the environment. The properties of WCO vary significantly from those of crude oils [6].

Recently, heterogeneous catalysts have demonstrated immense capability in generating biodiesel due to their elevated efficacy and abundant accessibility [7-9]. Moreover, it is asso-

ciated with the minimal expenditure of catalyst owing to its recyclability, the absence of effluent generation, low susceptibility to corrosion and easy washing methods. Homogeneous catalysts have certain drawbacks, like difficulty in the catalyst separation and extended time [10,11]. So, researchers have moved towards synthesizing biodiesel from cheap biodiesel feedstock and inexpensive heterogeneous catalysts involving simple and environment-friendly methods. As mentioned [12], using molybdenum oxide (MoOx) catalysts offers financial and environmental benefits. The present work examines the methyl ester synthesis derived from WCO utilizing ammonium molybdate and Li^+ loaded over eggshells-derived calcium oxide. CaO has been extensively used owing to its economical cost and alkaline nature and it is attainable from various raw materials. However, various problems persist that need to be addressed to enhance the catalytic characteristics of this substance. As an illustration, the catalytic regions might undergo deactivation or pollution through CO_2 and absorption of water molecules.

Additionally, the CaO regions exhibit diminished efficacy in unesterified fatty acids and have the potential to seep into the biodiesel, resulting in the formation of alkoxides that are regarded as effective in biodiesel production. However, leaching of CaO does contaminate the methyl ester content and reduces the recyclability of catalyst. The alkaline behaviour of the reactive regions is linked to the outer layer ions with weak coordination, which are susceptible to alteration through the calcination process [13]. Moreover, lithium is also introduced in the CaO framework to increase the alkalinity of calcium oxide. The material was confirmed by characterization techniques, *i.e.*, XRD, SEM and FTIR studies. Response surface methodology (RSM) was used in the experimental setup to optimize conditions for the highest biodiesel output.

EXPERIMENTAL

Ammonium molybdate tetrahydrate $(NH_4)_6Mo_7O_{24} \cdot 4H_2O$, methanol (99.0%) and anhydrous LiOH were procured from Rankem, India. Hexane (95%) was obtained from Sigma-Aldrich, USA. All reactants and solvents were employed without preceeding distillation. Waste cooking oil (WCO) was obtained from the canteen inside Banasthali premises and utilized as a raw material for methyl ester generation. The initial step involved filtering the WCO to eliminate the food impurities and then the WCO was heated to eliminate water particles. The saponification value, density, acid number and free fatty acid content (FFA) of the used cooking oil are specified in Table-1.

TABLE-1
PROPERTIES OF WASTE COOKING OIL (WCO)

Properties	Experiment value
Saponification value (mg KOH/g)	227
Density at 15 °C (kg/m³)	0.86
Free fatty acid (FFA, %)	0.84
Acid number (mg KOH/g)	1.68

Preparation of catalyst

Synthesis of calcium oxide from eggshells: The waste eggshells were initially cleaned with water and then desiccated

at 120 °C for 24 h. A mixer blender later pulverized the egg coverings into powdery form. The powdery substance was then calcinated for 3 h at 900 °C. Subsequently, the powder was immersed in water for 6 h. Following this, a drying span lasted 24 h at 120 °C. The obtained CaO was then heated for approximately 3 h at 600 °C through a calcination process and kept in storage for further utilization [14]. Then, a mixture was mixed by combining 10 g of CaO with 80 mL of distilled water followed by the addition of 10 mL of 1-4 wt.% ammonium molybdate solution. Then, 330 mg of LiOH were then introduced into the solution. The blend was agitated for 7 h at ambient temperature, further heated at 120 °C for an entire day and lastly subjected to calcination for 4 h at 700 °C [15].

The adequate duration of the calcination facilitates the even distribution of metal oxides with numerous reactive regions. Upon calcination, compounds from the raw materials and surface-bound molecules, such as water molecules, hydroxyl compounds and carbonated compounds, disintegrate from the specimen upon contact with the surroundings. Moreover, the metallic components in the unoccupied positions display an electron deficit and tend to be highly drawn toward oxygen atoms with excess electrons. The calcination temperature of 700 °C was chosen since molybdenum trioxide formation occurred at this particular temperature [16]. Navajas *et al.* [16] with MoO_3 and molybdenum oxide impregnated on alumina for biodiesel synthesis through transesterification of large unbound fatty acid levels present in oil, it was observed that MoO_3 was found as a blend of crystal structures (in both monoclinic and orthorhombic forms) at this particular temperature. Moreover, the porosity and surface properties were reported to be high when the samples were calcined at 700 °C. Supported MoOx catalyst materials and bulk molybdenum oxide possess Lewis and Brønsted acid functionalities. Still, they are significantly more prevalent and potent in reinforced catalyst materials because they can produce large biodiesel yields [17].

Catalyst characterization: XRD data was acquired from the X'Pert Pro instrument, employing CuKα radiation. The data collection spanned a 2θ range from 10º to 90º and the scanning speed was configured to 2º/min. The compounds were recognized by contrasting the obtained scattering patterns with the reference data. FTIR analysis was conducted using a spectrometer in 4000-400 cm⁻¹ region.

Transesterification procedure: The experiment occurred in a three-necked flask with a condensing unit, temperature gauge, oil bath and stirring magnet. The catalyst was introduced into the round bottom flask alongside the calculated quantity of methanol and then the mixture was stirred consistently. Then, 25 g of WCO was added into the blend and agitated at room temperature. For optimization, catalyst dose, time and the ratio of methanol:oil were varied for the highest response. The catalyst was subsequently separated through filter paper and any excess methanol was eliminated through heating. The filtered solution was decanted into the separatory funnel and stood uninterrupted for 24 h. The lower phase was discarded and the substance in the upper layer was washed with warm water. The conversion was calculated by applying the Knothe equation [18]:

$$\text{FAMEs yield (\%)} = \frac{2I(\text{methoxy})}{3I(\text{methylene})} \times 100$$

The integration measurements of methylene at 2.3 ppm and methoxy at 3.6 ppm are represented as $I_{(\text{methylene})}$ and $I_{(\text{methoxy})}$, respectively [19].

Experimental design and data analysis: The synergistic impacts of various parameters in the transesterification reaction were investigated. These parameters included reaction time (spanning 30 to 120 min), catalyst concentration (ranging from 2-8 wt.%) and the alcohol to oil ratio (ranging from 8.14-16.02 m/m). This exploration was conducted utilizing a statistical method. Central Composite Design (CCD) was used in the experimental setup to optimize conditions for the highest biodiesel output. The factors considered for this design were the molar ratio of m/o (labelled as 'A'), catalyst dose (labelled as 'B') and the duration of the reaction (labelled as 'C') (Table-2). These three factors served as independent inputs. The Design Expert software determined two α values at their highest points. These values represent the parameter's extremes: one corresponds to the smallest value, *i.e.* (-) α and the other corresponds to the largest value, *i.e.* (+) α. The trial version of Stat-Ease software was employed for various analytical tasks. The accuracy of the expected model was assessed *via* analysis of variance (ANOVA). In this process, the obtained values were expected to align in a linear pattern on the normal probability plot.

RESULTS AND DISCUSSION

Catalyst analysis

XRD studies: The X-ray structural analysis patterns of eggshells derived from CaO, Li/CaO and 1-4 wt.% Mo impregnated Li/CaO are depicted in Fig. 1. The strong diffraction peaks at 2θ values of 34.74°, 47.56°, 51.56°, 29.13° and 18.56° confirmed the presence of CaO. The peak at a 2θ value of 50.86° indicated that the impregnation of lithium distorts the CaO structure. For molybdenum content reaching 2 wt.%, the impregnation onto Li/CaO support revealed faint diffraction patterns. This occurrence underscores the effective distribution of molybdenum species over the Li/CaO support. A 1% Mo/Li-CaO catalyst demonstrated almost the same diffractograms in contrast to 2, 3 and 4% Mo/Li-CaO catalysts. At 1 wt.% and 3 wt.%, an intense peak was seen at 2θ values of 54.35°, which showed the formation of CaMoO₄ species and larger particle dimensions. This indicated that the infusion of Mo elevated the crystalline arrangement of the Li-CaO catalyst. The peak intensity was reduced at high molybdenum loading of 4 wt.% due to diminished acidic site availability, confirming its low reactivity towards transesterification reaction. It was also observed that 2θ values at 18.6°, 10.7° and 34.2° were absent, corresponding to ammonium
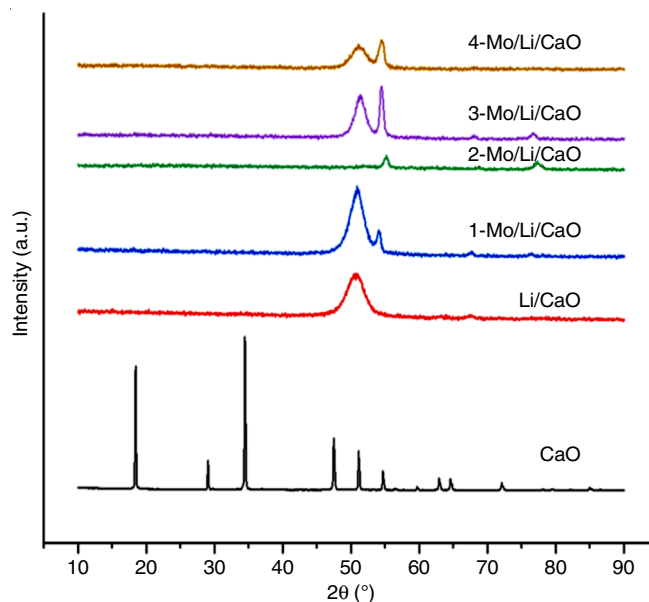
Fig. 1. XRD patterns of CaO, Li/CaO and 1-4 wt % Mo/Li/CaO

molybdate species (JCPDS card no. 23-0784) in the calcined samples.

SEM studies: Fig. 2a-b depicts the SEM image at different magnifications of the 3-Mo/Li-CaO catalyst. A strong and erratic distribution of aggregates without distinct forms was observed.

FTIR studies: The FTIR analysis was conducted to identify the chemical moieties contained in the synthesized catalysts. The FTIR spectral of CaO, Li/CaO and 3-Mo/Li/CaO are shown in Fig. 3a-c. The infrared spectral band at 876.59 and 1422.87 cm⁻¹ aligns with the resonance of carbonate ion (CO_3^{2-}). The bands at 3637.29, 3747.44 and 3641.81 cm⁻¹ represent the absorption of H_2O. The band at 637.66 cm⁻¹ relates to Li-O bond stretching. The bands at 1694.06 and 2365.63 cm⁻¹ validated the existence of lithium and the band at 869.76 cm⁻¹ confirmed the loading of Mo on the Li/CaO support.

Catalyst's performance

Impact of impregnated molybdenum species concentration: Several catalysts were synthesized with molybdate species ranging from 1-4 wt.% to identify the ideal molybdenum amount for Mo/Li/CaO reactivity. The transesterification process was conducted at 60 °C for 1 h employing a ratio of m/o of 13.70:1 and 4 wt.% catalyst dose. The performance of catalyst was enhanced with increased Mo amount to 3 wt.%. An additional increase in the Mo loading (4 wt.%) lowers the catalytic activity. Hence, 3 wt.% was chosen as the optimal loading of molybdenum (Fig. 4). The XRD also confirmed that increasing molybdenum loading beyond 3% diminishes the peak intensity at a 2θ value of 54.35°, thus reducing catalytic activity in the

TABLE-2
DESIGNATED INTERVAL AND DISTINCT FIGURES OF THE INDEPENDENT VARIABLES WERE UTILIZED IN THE CENTRAL COMPOSITE DESIGN

Name	(-) α	Minimum	Maximum	(+) α
Ratio of methanol:waste cooking oil (A) (m/m)	5.4374	8.14	16.02	18.7063
Catalyst dose (B) (wt.%)	-0.0453785	2	8	10.0454
Time (C) (min)	-0.680677	30	120	150.681
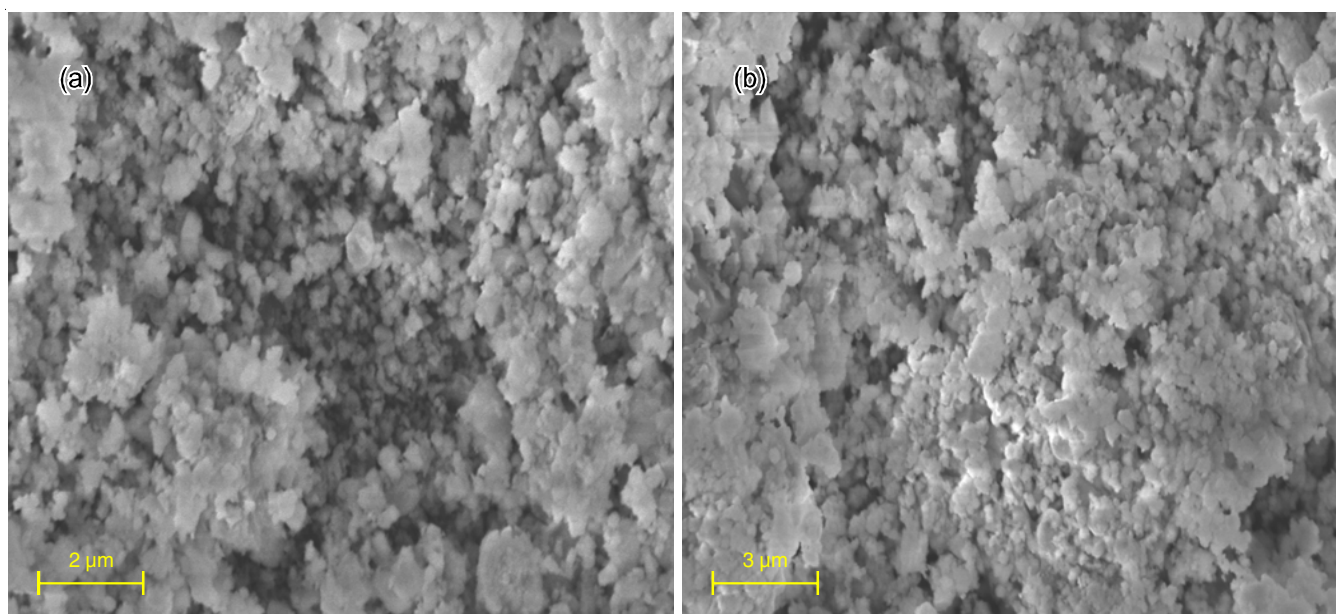
Fig. 2. SEM image at different magnifications of the 3-Mo/Li/CaO catalyst

transesterification reaction. The higher molybdenum loading obstructs the catalytic centers on the Li/CaO support, which profoundly impacts the response.

Response surface methodology (RSM) optimization: The three-dimensional plots were generated utilizing the quadratic function derived from the regression analysis of experimental outcomes. This was achieved by maintaining a constant temperature and one of the input variables while varying the other two variables. Reactions were carried out following the CCD methodology using Design Expert. This involved changing input factors like the m/o ratio (labelled as 'A'), catalyst dose (labelled as 'B') and the duration of the reaction (labelled as 'C'). The aim was to assess their influence on the production of biodiesel. A total of 15 runs were used to determine the three factors involved in the reaction, keeping one constant, *i.e.* temperature. The factors encompass the reaction duration (spanning 0.5 to 2 h), catalyst concentration (ranging from 2 to 8 wt.%) and the m/o ratio (ranging from 8.14 to 16.02 m/m). The temperature was controlled at 60 ºC across all runs and the model showed statistically significant results (Table-3).

The regression model ideally reveals the connection between the observable and explanatory factors. The viability of examining the impact of variables backed by the empirical data is effectively demonstrated in this model. Following numerous attempts to fit the observed data into regression functions, formulated analytical tools with a straight-line interplay of operational variables yielded inadequate fit with a deficient value of determination coefficient, rendering it incapable of elucidating the entire empirical dataset. Ultimately, the polynomial model with a linear relationship of operational variables was deemed suitable after assessing a range of potential models and the best-fit regression formulation derived from the empirical observations. The empirical data underwent several regression assessments to ensure a precise prediction of the possible biodiesel quantity, culminating in the formulation of a non-linear fitting equation as displayed in eqn. 1. The reliability of model was assessed utilizing the determination coefficient (R^2), resulting in a value of 0.9882, as depicted in Table-4. It suggested that the proposed model accounts for 98.82% of observed data, with a less than 2% of the overall discrepancies in the equation

	TABLE-3					
	MODEL-PREDICTED AND OBSERVED DATA OF BIODIESEL RESPONSE					
Origin	Summation of squares	Degree of freedom	Average square	Fischer F-ratio	P-value	
Model	2930.84	9	325.65	61.15	0.0031	Significant
A-Ratio of m/o	176.12	1	176.12	33.07	0.0104	
B-Catalyst amount	694.67	1	694.67	130.44	0.0014	
C-Reaction duration	1120.23	1	1120.23	210.35	0.0007	
AB	435.12	1	435.12	81.70	0.0029	
AC	36.12	1	36.12	6.78	0.0801	
BC	28.12	1	28.12	5.28	0.1052	
A^2	7.23	1	7.23	1.36	0.3282	
B^2	0.71077	1	0.7107	0.1334	0.7391	
C^2	0.7831	1	0.7831	0.1470	0.7269	
Residual	15.98	3	5.33			
Cor total	2946.81	12				
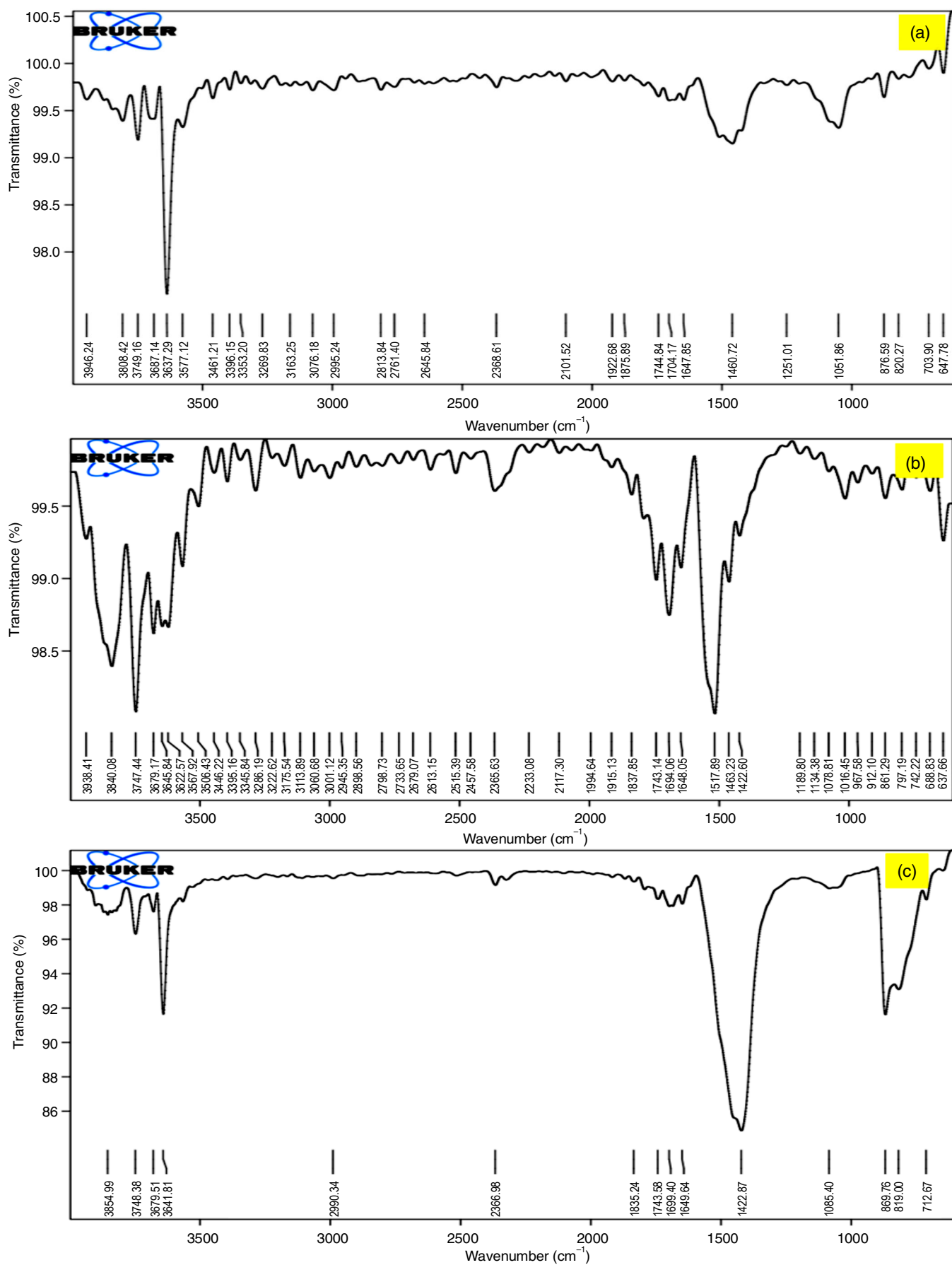
Fig. 3. FTIR spectra of (a) CaO, (b) Li/CaO and (c) 3-Mo/Li/CaO
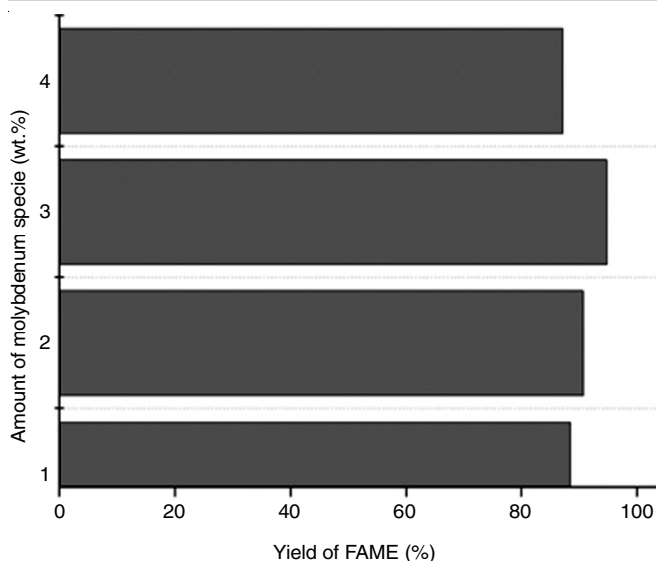
Fig. 4. Effect of the amount of molybdenum species on the yield of biodiesel

TABLE-4
FORECASTED AND MODIFIED R^2 VALUES OF THE MODEL

Std. Dev.	2.41	R^2	0.9882
Mean	74.03	Adjusted R^2	0.9763
C.V. %	3.26	Predicted R^2	0.9448

remaining unaccounted for. The adjusted determination coefficient of 0.9763 was obtained and this value reflects the effectiveness of the formulated experimental model.

The goodness of fit or determination coefficient (R^2) is a numeric indication of the appropriateness of aligning the graphs in straight-line analysis. The suitability of the fit becomes less informative of the statistical analysis findings as the coefficient of determination analysis reaches the minimum value of 0. When the R-squared value is close to 1, it characterizes the data sets closely aligned with the straight line and is considered to represent the optimal interaction among the variables. The regression model F-test suggested that the model is statistically vital. It is evident that the factors within the linear variables involving catalyst dose (B) and time (C) significantly influence the FAME yield, attributed to their highest Fisher's F-ratios/F-values. A^2 (ratio of m/o) has the highest F-value, succeeded by C^2 (time) and B^2 (catalyst dose). The impact of time, catalyst dose and ratio of m/o on FAME response is strongly indicated to be illustrated through the linear factors due to the elevated F-values.

Similarly, the collaborative factor involving catalyst dose and the ratio of methanol to oil (AB) demonstrated significant impacts on biodiesel response due to a high F-value of 81.70, in contrast to the collaborative factor involving the m/o ratio and time (AC) and catalyst dose-time (BC). The linear factor of time displayed the most substantial numeric factor, suggesting its robust influence on biodiesel response, followed by B (catalyst amount) and A (ratio of m/o). The second-order coefficient, A^2, the linear term (C) and collaborative factors AC, AB and BC negatively affected the biodiesel yield. The p-value provides insights into the significance and magnitude of a mathematical hypothesis. A lower p-value signifies the statistical significance

of single model parameters, with the least value represented by (C), the linear factor of time, emphasizing that the variable holds the utmost significance in contrast to other variables. Matching numeric factors are deemed significant if the p-value is below 0.05. The squared factors in this model, A^2, B^2 and C^2 with collaborative factors AC, AB and BC, emerged as insignificant model factors due to their p-values greater than 0.05. Consequently, the predominant variable identified is time, denoted as C, presenting the highest negative coefficient in the square polynomial equation, the highest Fischer F-ratio and the most minimal P-value.

$$Y = 74.83 + 3.59\,A + 8.92\,B - 11.33\,C - 1.12\,A^2 + 0.4004\,B^2 + 0.4203\,C^2 - 7.37\,AB - 2.12\,AC - 1.87\,BC \tag{1}$$

Y represents FAME response, with A, B and C symbolizing the ratio of methanol:waste cooking oil, catalyst dose and time. AC, AB and BC represent combined impacts; A^2, B^2 and C^2 represent second-order variables. A positive coefficient in the quadratic formula signifies a collaborative influence. It means the outcome increases with the rise in the value of explanatory variables. Conversely, a minus sign indicates the inverse effect, where the output enhances as the value of the input variable lowers.

Fig. 5 shows the typical probability plot. The residuals align in a linear pattern indicated that the inaccuracies conform to a normal distribution and demonstrate the suitability of the non-linear regression model. Fig. 6 illustrates a graphical comparison between the outcomes of actual transesterification experiments and the results anticipated by the software. The graph highlights a significant alignment between the essential data entries and the projected values as evidenced by the response values closely following the diagonal line. This close correlation indicates a substantial concurrence between the empirical data and the projections generated by the software signifying a robust agreement.
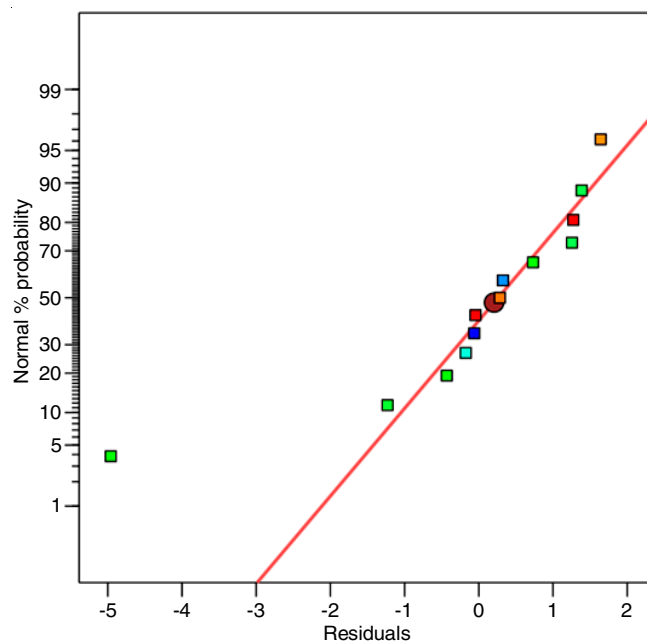
Fig. 5. Normal probability plot
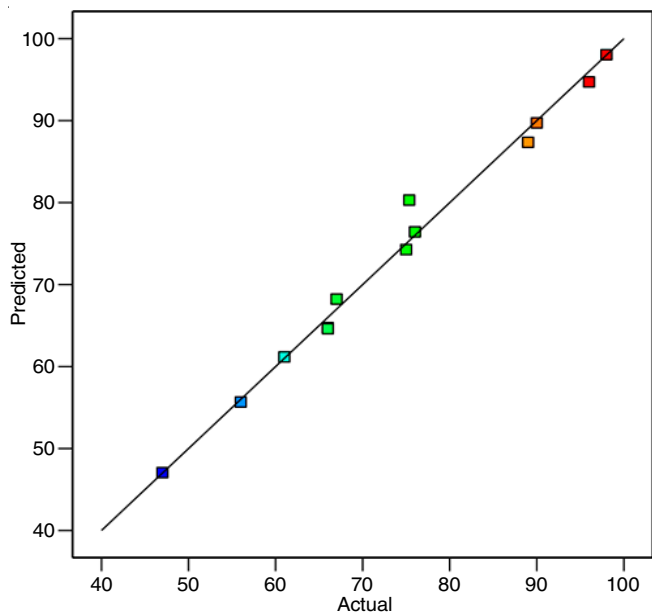
Fig. 6. A comparison between actual and predicted values

Fig. 7 represents the 3D and interaction graph of biodiesel yield with catalyst dose and ratio of methanol:oil produced by the Design Expert tool. The stoichiometric proportion of alcohol: oil is a fundamental variable influencing the biodiesel yield, aiming to improve the effects of blending and thermal exchanges. The coefficients of the transesterification reaction distinctly show that 3 moles of alcohol are required for each single mole of lipid. Still, the biodiesel generation process necessitates more alcohol to drive the biodiesel production. The biodiesel yield increased as the catalyst dose and proportion of methanol to oil increased. This is due to the favourable impacts these variables exert on the outcome. The FAME yield increased with the increase in catalyst dose owing to rise in reactive regions. Given the reaction for biodiesel production can occur in a reverse direction enhancing the quantity of alcohol results in a large yield of biodiesel.

However, an escalation in the magnitudes of the factors after a specific point results in a marginally decreased value of biodiesel production. Excess solvent (methanol) hinders the segregation of biodiesel and glycerol, reducing biodiesel output. Additional methanol weakens the strength of the alcohol (methanol) and the waste cooking oil, consequently diminishing the reaction rate. The monoacyl and diacyl glycerides can blend the stages of biodiesel, alcohol and glycerol enhancing the backward reaction and diminishing the response.

The ratio of waste cooking oil to methanol remained consistent at 1:12.08 to investigate the mutual influence of variables (B and C). By enhancing the catalyst dose, the production output of biodiesel was improved due to an increased number of reactive species, which enhances the reaction rate (Fig. 8). Using a smaller amount of catalyst in the transesterification reaction might lead to a reduced surface area, which in turn leads a decrease in the biodiesel response. Similar results were obtained with CaO-MgO catalyst employed in the methyl ester production from non-edible oil; the maximum biodiesel response of 93.55% was attained with 3.70 wt.% (catalyst), 115.87 °C (temperature), 3.44 h (time) and 38.67:1 (ratio of m/o)
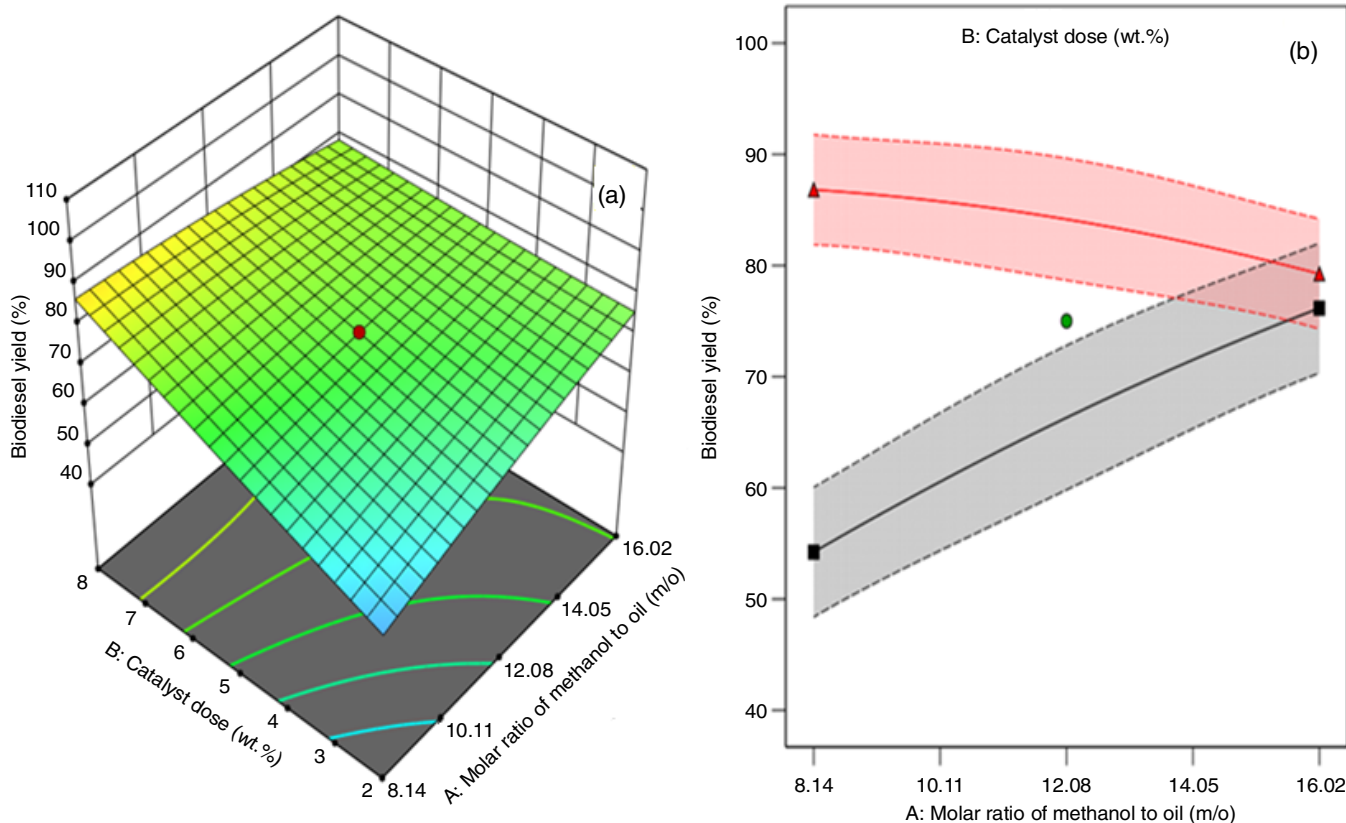
Fig. 7. (a) Three-dimensional and (b) Interaction graph of biodiesel yield with catalyst dose and m/o ratio
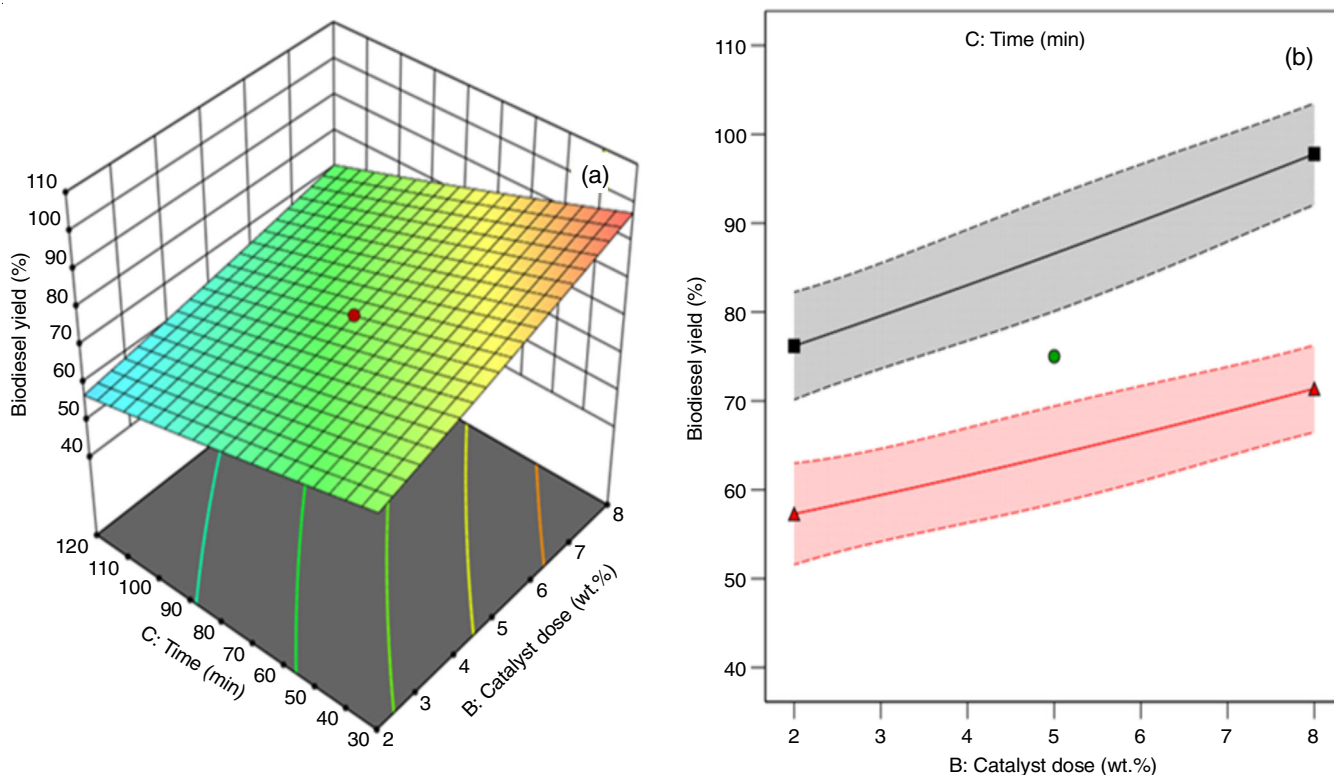
Fig. 8. (a) Three-dimensional and (b) Interaction graph of biodiesel yield with catalyst dose and reaction duration

[20]. Throughout the reaction duration, the FAME yield was diminished due to the initiation of a backward process. This could suggest that the reaction achieved a state of equilibrium at 60 min. Beyond this value, there was a negligible impact on the biodiesel response.

Fig. 9 shows the three-dimensional and interaction graph of biodiesel yield with reaction duration and the ratio of m/o. The duration and m/o ratio impact was determined by maintaining the catalyst dose at the mid-value (5 wt.%). An increase in the ratio of m:o increases the FAME production when the time is small. At minimum reaction time (30 min) and highest ratio of alcohol to oil (16.02:1), a large FAME response was observed. Moreover, with an increase or decrease in temperature, the rising value of the ratio of ethanol to cottonseed oil had a negligible impact on oil conversion to biodiesel. Increasing the reaction duration reduced the performance. The optimal reaction duration obtained in the present study is 1 h.

Characterization of biodiesel

^{1}H and ^{13}C NMR studies: The ^{13}C and ^{1}H NMR spectra of the produced FAME are displayed in Fig. 10. The signal at δ 3.67 ppm validates the formation of fatty acid methyl ester, while a resonance at δ 2.23 ppm emerged for methylene proton signals [21]. The allylic protons resonated at 2-2.1 ppm; alkenes exhibited signals. In δ 5.3-5.4 ppm range, diallyl carbons resonated at δ 2.7-2.8 ppm. The aliphatic methyl esters were identified through the alkyl CH$_2$ protons resonating in the δ 1.2-1.4 ppm range. In ^{13}C NMR of WCO biodiesel, the peaks at δ 174.06 ppm and δ 129.86 ppm confirmed methyl ester formation and the existence of unsaturation in ester. A peak at δ 13.98 ppm

indicated the terminal methyl carbon [22]. The distinct signal of the lack of peaks between δ 3.9 and δ 4.5 ppm suggests the absence of glycerol.

GC-MS studies: The GC-MS was performed to evaluate the constituents of methyl ester. The existing reference data identified the peaks of produced biodiesel. The sample was inspected with an inert 5975 mass-selective detector for every examination. The capillary column containing 5% phenyl and 95% dimethylpolysiloxane was employed with He as a carrier gas. The column's thermal profiling is specified, initiating subjecting to heating at 160 ℃ for 3 min followed by the commencement of temperature increasing from 160-230 ℃, with an advancing temperature gradient of 5 ℃/min. It was observed that methyl ester hexadecanoic acid has the most significant peak area value of 50.80% (Table-5). The primary components of biodiesel were hexadecanoic acid methyl ester, methyl 9,12-octadecadienoic acid ester, cis-9-octadecenoic acid methyl ester, stearic acid methyl ester, methyl docosanoate, methyl eicosanoate, methyl octanoate, methyl tetracosanoate, methyl cis-11-eicosenoic acid ester and methyl cis-epoxyoctanoate at retention time (RT) of 18.51, 20.51, 21.25, 21.33, 25.05, 23.04, 7.48, 23.37, 22.79 and 22.57, respectively. Fig. 11 shows the relative abundance of methyl esters with time.

Reusability studies of catalyst: Leveraging a heterogeneous catalyst in biodiesel production offers a significant benefit in catalyst reusability, which minimizes the production cost of biodiesel [23]. Studying catalyst reusability helps predict the financial viability of commercial-scale methyl ester synthesis. The synthesized 3-Mo/Li/CaO catalyst was recycled at the optimized reaction conditions. After each cycle, the catalyst
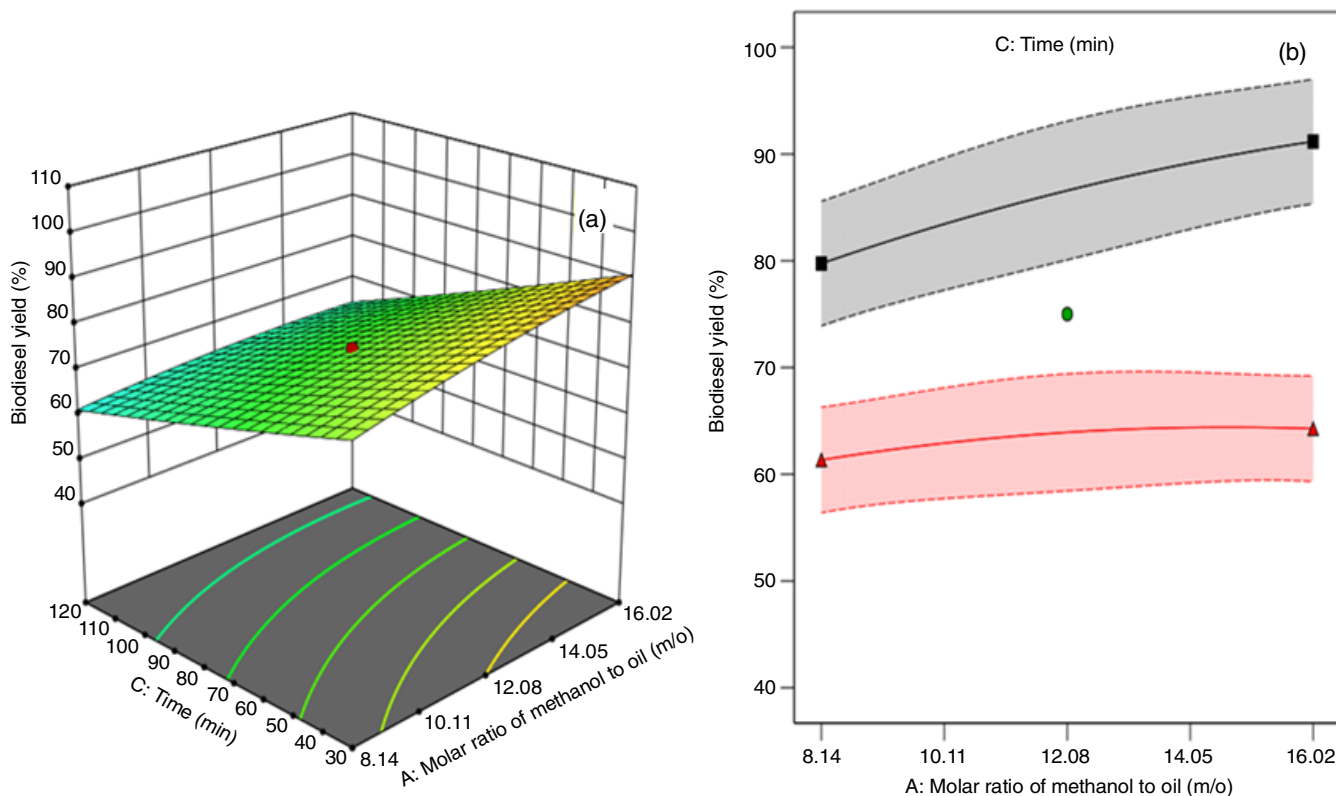
Fig. 9. (a) Three-dimensional and (b) Interaction graph of biodiesel yield with ratio of methanol:oil and reaction duration
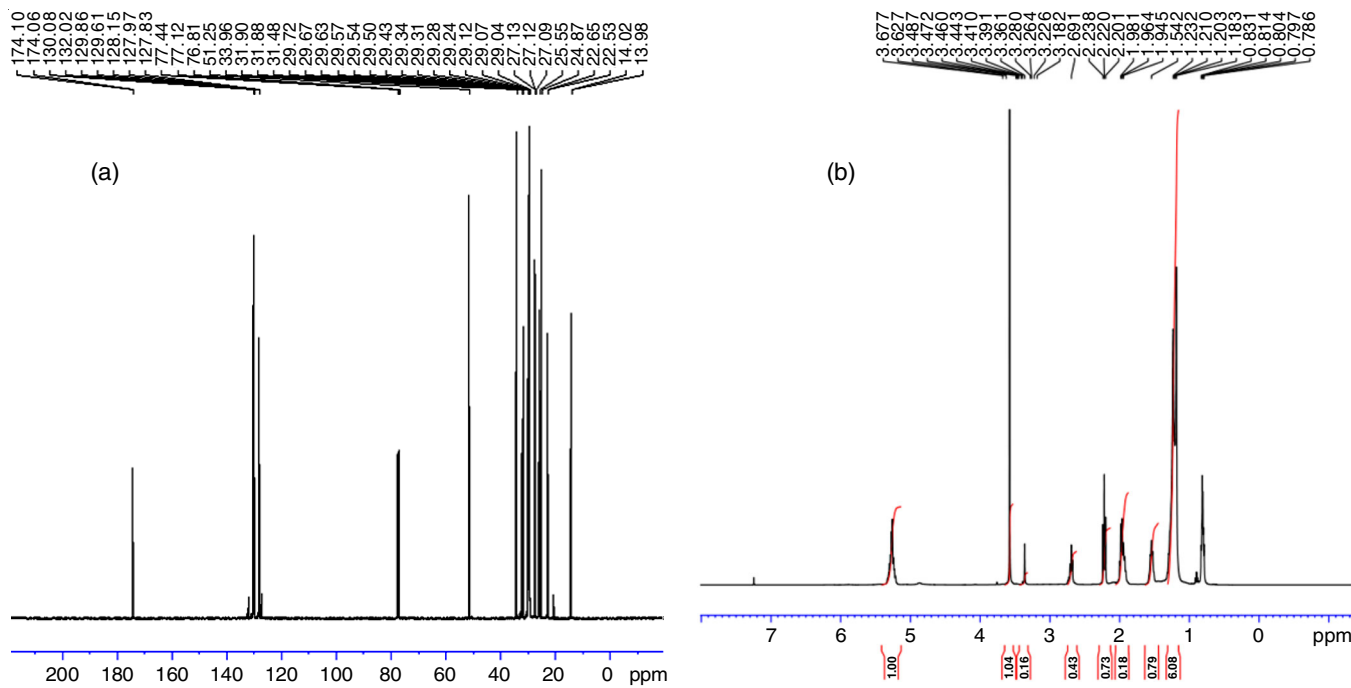
Fig. 10. ^{13}C NMR (a) and ^{1}H NMR (b) spectra of synthesized biodiesel

was washed with *n*-hexane to remove impurities, remaining glycerol and residual methanol. This washing was performed three times to ensure complete elimination of glycerol. It was then desic-cated at 120 ºC and calcined at 700 ºC for 3 h. This empirical observation suggests that the synthesized catalyst can be restored and effectively employed for industrial biodiesel manufacturing. The production output diminished after 5 cycles from 97% to 56.2%. This reduction in the catalytic efficacy of catalyst can be ascribed to the leaching of lithium ions and entrapment of the organic substances in porous framework. It may be attributed to catalyst loss after the 5th cycle and disso-lution of molybdenum species existing within Li/CaO [16].

TABLE-5
COMPOSITION OF WASTE OIL-DERIVED BIODIESEL

RT	Name of the compound	m.f.	m.w.	Peak area (%)
18.51	Methyl hexadecanoate	$C_{17}H_{34}O_2$	270	50.80
20.51	Methyl 9,12-octadecadienoate	$C_{19}H_{34}O_2$	294	19.78
21.25	Methyl *cis*-9-octadecenoate	$C_{19}H_{36}O_2$	296	17.28
21.33	Stearic acid methyl ester	$C_{19}H_{38}O_2$	298	6.89
25.05	Methyl docosanoate	$C_{23}H_{46}O_2$	354	2.36
23.04	Methyl eicosanoate	$C_{20}H_{40}O_2$	312	1.28
7.48	Methyl octanoate	$C_9H_{18}O_2$	158	0.42
23.37	Methyl tetracosanoate	$C_{22}H_{44}O_2$	340	0.41
22.79	Methyl *cis*-11-eicosenoate	$C_{21}H_{40}O_2$	324	0.40
22.57	Methyl *cis*-epoxyoctanoate	$C_{25}H_{42}O_2$	374	0.36
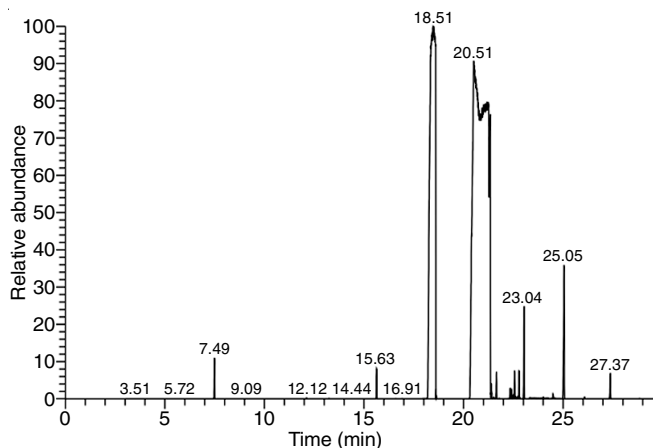
Fig. 11. Plot of relative abundance with time

Conclusion

A wet impregnation method to prepare a 3-Mo/Li/CaO as catalyst for transesterification of waste cooking oil (WCO) for biodiesel synthesis. The catalyst was characterized with XRD, SEM and FTIR techniques. The performance of the prepared catalyst was enhanced with the rise in Mo amount to 3 wt.%. The XRD also confirmed that an increase in the molybdenum loading beyond 3% diminishes the peak intensity at a 2θ value of 54.35°, resulting in the lower catalyst efficiency towards the reaction. Higher molybdenum loading obstructs the catalytic centers on the Li/CaO support, which profoundly impacts the biodiesel response. At 60 °C and a catalyst loading of 6 wt.% with a ratio of methanol to oil (m/o) of 13.70:1, took 1 h for 3-Mo/Li/CaO to produce the maximum output of biodiesel. The reaction parameters were fine-tuned using regression analysis. The factors encompass the reaction duration (spanning 30 to 120 min), catalyst concentration (ranging from 2 to 8 wt.%) and the m/o ratio (ranging from 8.14 to 16.02 m/m). A significant comparison among the actual data and the projected values of the transesterification reaction with the determined coefficient (R^2) value of 0.988 was observed. The reusability of catalyst was good and the catalyst can be reutilized effectively up to a limit of 5 runs.

REFERENCES

1. A. Lancheros, O. Brito and M.F. Guimarães, *Remediat. J.*, **34**, e21769 (2023);
    https://doi.org/10.1002/rem.21769
2. N. Zou, X. Lin, M. Li, L. Li, C. Ye, J. Chen and T. Qiu, *ACS Sustain. Chem. & Eng.*, **8**, 18054 (2020);
    https://doi.org/10.1021/acssuschemeng.0c06139
3. S.H. Park, N. Khan, S. Lee, K. Zimmermann, M. DeRosa, L. Hamilton, W. Hudson, S. Hyder, M. Serratos, E. Sheffield, A. Veludhandi and D.P. Pursell, *ACS Omega*, **4**, 7775 (2019);
    https://doi.org/10.1021/acsomega.9b00268
4. R. Karmakar, A. Rajor, K. Kundu and N. Kumar, *Petrol. Sci.*, **15**, 164 (2018);
    https://doi.org/10.1007/s12182-017-0203-0
5. S. Di Fraia, N. Massarotti, M.V. Prati and L. Vanoli, *Energy Convers. Manage.*, **211**, 112763 (2020);
    https://doi.org/10.1016/j.enconman.2020.112763
6. W.H. Foo, W.Y. Chia, D.Y.Y. Tang, S.S.N. Koay, S.S. Lim and K.W. Chew, *J. Hazard. Mater.*, **417**, 126129 (2021);
    https://doi.org/10.1016/j.jhazmat.2021.126129
7. Y. Guo, S.A. Delbari, A.S. Namini, Q.V. Le, J.Y. Park, D. Kim, R.S. Varma, H.W. Jang, A. T-Raissi, M. Shokouhimehr and C. Li, *Mol. Catal.*, **547**, 113362 (2023);
    https://doi.org/10.1016/j.mcat.2023.113362
8. B. Changmai, C. Vanlalveni, A.P. Ingle, R. Bhagat and S.L. Rokhum, *RSC Adv.*, **10**, 41625 (2020);
    https://doi.org/10.1039/D0RA07931F
9. S.P. Gouda, A. Dhakshinamoorthy and S.L. Rokhum, *Chem. Eng. J. Adv.*, **12**, 100415 (2022);
    https://doi.org/10.1016/j.ceja.2022.100415
10. A.L. Silva, A.F.F. Farias, J.B. Costa Agra de Melo, A.M. Rodrigues, S.M.P. Meneghetti and A.C.F. Melo Costa, *Int. J. Energy Res.*, **46**, 7775 (2022);
    https://doi.org/10.1002/er.7679
11. T.V. dos Santos, N. dos Santos Brainer, D.B. de Amorin Pryston, D.O. da Silva Avelino, C.B. Dornelas, M.R. Meneghetti and S.M.P. Meneghetti, *Catal. Lett.*, **149**, 3132 (2019);
    https://doi.org/10.1007/s10562-019-02869-6
12. S. Muthamizh, C. Sengottaiyan, R. Jayavel and V. Narayanan, *J. Nanosci. Nanotechnol.*, **20**, 2823 (2020);
    https://doi.org/10.1166/jnn.2020.17456
13. D. Olvera, J.A. Rodriguez, I. Perez-Silva, G. Chavez-Esquivel and J.A. Tavizon-Pozos, *Chem. Zvesti*, **76**, 6287 (2022);
    https://doi.org/10.1007/s11696-022-02305-x
14. A. Hameed, S.R. Naqvi, U. Sikandar and W.-H. Chen, *Catalysts*, **12**, 592 (2022);
    https://doi.org/10.3390/catal12060592

15. I. Ambat, V. Srivastava, E. Haapaniemi and M. Sillanpää, *Sustain. Energy Fuels*, **3**, 2464 (2019);
https://doi.org/10.1039/C9SE00210C

16. A. Navajas, I. Reyero, E. Jiménez-Barrera, F. Romero-Sarria, J. Llorca and L.M. Gandía, *Catalysts*, **10**, 158 (2020);
https://doi.org/10.3390/catal10020158

17. A.L. Silva, A.F.F. Farias, S.M.P. Meneghetti, E.A. dos Santos Filho and A.C.F. de Melo Costa, *Arab. J. Chem.*, **15**, 104012 (2022);
https://doi.org/10.1016/j.arabjc.2022.104012

18. G. Knothe, *J. Am. Oil Chem. Soc.*, **83**, 823 (2006);
https://doi.org/10.1007/s11746-006-5033-y

19. M. Balajii and S. Niju, *Renew. Energy*, **146**, 2255 (2020);
https://doi.org/10.1016/j.renene.2019.08.062

20. H.V. Lee, R. Yunus, J.C. Juan and Y.H. Taufiq-Yap, *Fuel Process. Technol.*, **92**, 2420 (2011);
https://doi.org/10.1016/j.fuproc.2011.08.018

21. M. Hossain, N. Muntaha, L.K.M.O. Goni, M.S. Jamal, M.A. Gafur, D. Islamand A.N.M. Fakhruddin, *ACS Omega*, **6**, 35679 (2021);
https://doi.org/10.1021/acsomega.1c05582

22. S. Ishak and A. Kamari, *Environ. Chem. Lett.*, **17**, 1143 (2019);
https://doi.org/10.1007/s10311-018-00844-y

23. I.M. Mendonça, O.A.R.L. Paes, P.J.S. Maia, M.P. Souza, R.A. Almeida, C.C. Silva, S. Duvoisin Jr. and F.A. de Freitas, *Renew. Energy*, **130**, 103 (2019);
https://doi.org/10.1016/j.renene.2018.06.059